*Journal of the European Ceramic Society* **10** (1992) 453–459

# Zirconia Stabilized with a Mixture of the Rare Earth Oxides

W. Pyda, K. Haberko*

Academy of Mining and Metallurgy, Department of Special Ceramics, Cracow, Al. Michiewicza 30, Poland

&

Z. Żurek

Cracow Polytechnic, Institute of Chemistry and Inorganic Technology, Cracow, ul. Warszawska 24, Poland

(Received 28 October 1991; revised version received 28 January 1992; accepted 28 February 1992)

***Abstract***

*A hydrothermal technique was used to prepare micropowders of $ZrO_2$ solid solutions stabilized by the mixture of rare earth oxides and yttria ($Ln_2O_3$) recovered from phosphogypsum. Phase compositions and particle sizes of the powders were measured. Zirconia solid solutions of cubic and tetragonal symmetry are the major phases. A larger $Ln_2O_3$ concentration promotes a greater cubic phase content. Powders having low $Ln_2O_3$ concentrations have small amounts of monoclinic phase present.*

*The phase composition, fracture toughness ($K_{Ic}$) and Vickers hardness of samples sintered at temperatures ranging from 1250 to 1350°C were measured. Tetragonal and, in some cases, monoclinic zirconia solid solutions are found in the microstructure of the sintered bodies. Two ordered phases with the formulae $Ln_2Zr_2O_7$ and $Ce_2Zr_3O_{10}$ were also detected in the system. Tetragonal zirconia polycrystals (TZP) with high ($10\ MPa\ m^{0.5}$) fracture toughness were found.*

*Es wurde eine hydrothermische Methode angewandt, um $ZrO_2$-Mikropulver herzustellen, die durch ein Gemisch von Seltenen Erd-Oxiden und Yttriumdioxid ($Y_2O_3$) stabilisiert wurden und mit Phosphat-Gips eingehüllt wurden. Die Phasenzusammensetzungen und die Teilchengrößen der Pulver wurden bestimmt. Die Hauptphasen sind kubisches und tetragonales Zirkoniumdioxid. Ein höherer Gehalt an $Y_2O_3$ führt zu einem höheren kubischen Phasenanteil. Pulver mit geringerem $Y_2O_3$-Anteil zeigen geringe Gehalte an monokliner Phase.*

*Die Phasenzusammensetzungen, die Bruchzähigkeit ($K_{Ic}$) und die Vickers-Härte bei Temperaturen zwischen 1250 und 1350°C gesinterter Proben wurden bestimmt. Tetragonales und in einigen Fällen auch monoklines Zirkoniumdioxid können im Gefüge gesinterter Proben beobachtet werden. Zwei geordnete Phasen mit den Stöchiometrien $Ln_2Zr_2O_7$ und $Ce_2Zr_3O_{10}$ wurden ebenfalls im System entdeckt. Tetragonale Zirkoniumdioxid-Vielkristalle (TZP) mit hoher Bruchzähigkeit ($10\ MPa\ m^{0.5}$) wurden beobachtet.*

*Une technique hydrothermique a été utilisée pour préparer une micro-poudre de $ZrO_2$ stabilisée par un mélange d'oxydes de terre rare ($Ln_2O_3$) et d'oxydes d'yttrium ($Y_2O_3$) recouverts par du phosphate de gypse. On a étudié les compositions des phases ainsi que la taille des particules. On a trouvé que la zircone de symmétrie cubique et tétragonale forme la majorité des phases. On a remarqué que l'utilisation de $Ln_2O_3$ en forte concentration favorise la formation de la phase cubique et que les poudres ayant $Ln_2O_3$ en faible concentration présentent une faible quantité de phase monoclinique.*

*On a étudié la composition des phases, la ténacité ($K_{Ic}$) ainsi que la dureté Vickers sur des échantillons frittés entre 1250 et 1350°C. De la zircone tétragonale et dans certains cas de la zircone monoclinique ont été trouvées dans la microstructure des produits frittés. En outre, deux phases crystallines ayant pour formule $Ln_2Zr_2O_7$ et $Ce_2Zr_3O_{10}$ ont été aussi détectées. Les*

* To whom correspondence should be addressed.



*Journal of the European Ceramic Society* 0955-2219/92/$5.00 

*polycristaux de zircone tétragonale (TZP) observés, possèdent une forte ténacité (10 MPa m$^{0.5}$).*

## 1 Introduction

During the last 15 years several systems suitable for the preparation of tetragonal zirconia polycrystals of good mechanical properties have been investigated. These are following: $Y_2O_3$–$ZrO_2$,[1–3] $CeO_2$–$ZrO_2$,[4–7] CaO–$ZrO_2$,[8] MgO–$Y_2O_3$–$ZrO_2$,[9–11] CaO–$TiO_2$–$ZrO_2$,[12] $TiO_2$–$Y_2O_3$–$ZrO_2$.[13–16]

The aim of the present work was to study the possibility of the application of a mixture of rare earth oxides and yttria recovered during phosphogypsum processing to the stabilization of tetragonal zirconia polycrystals. The chemical composition of the stabilizing mixture is given in Table 1. According to these data $CeO_2$, $La_2O_3$ and $Nd_2O_3$ are the main components of the mixture.[17]

## 2 Experimental

A hydrothermal technique was used to prepare the starting powders.[18] The first step of the process consists of the coprecipitation of the mixed hydroxides of zirconium and the elements shown in Table 1. This was accomplished by introducing the mixed solution of zirconyl chloride and nitrides of the stabilizing cations into the vigorously stirred ammonium hydroxide solution. The final pH of 9 was maintained to obtain quantitative coprecipitation. The resulting gel was washed with distilled water to remove the remaining ammonium salts and subsequently hydrothermally treated under the autogeneous water vapour pressure at 250°C for 4 h.

**Table 1.** Rare earth oxide mixture analysis[17]

| *Element* | *Content (wt%)* | *Oxide* | *Content (mol%)* |
|---|---|---|---|
| Y | 1·9 ± 0·5 | $Y_2O_3$ | 2·58 ± 0·68 |
| La | 22·5 ± 0·9 | $La_2O_3$ | 19·59 ± 0·78 |
| Ce | 37·0 ± 2·0 | $CeO_2$ | 63·9 ± 3·5 |
| Pr | 3·0 ± 0·2 | $Pr_2O_3$ | 2·57 ± 0·17 |
| Nd | 10·5 ± 0·5 | $Nd_2O_3$ | 8·80 ± 0·42 |
| Sm | 1·13 ± 0·05 | $Sm_2O_3$ | 0·909 ± 0·040 |
| Eu | 0·329 ± 0·008 | $Eu_2O_3$ | 0·261 8 ± 0·006 4 |
| Gd | 0·79 ± 0·07 | $Gd_2O_3$ | 0·608 ± 0·054 |
| Tb | 0·960 ± 0·007 | $Tb_4O_7$ | 0·365 3 ± 0·002 7 |
| Dy | 0·323 ± 0·004 | $Dy_2O_3$ | 0·240 4 ± 0·003 0 |
| Ho | 0·049 ± 0·01 | $Ho_2O_3$ | 0·035 9 ± 0·007 3 |
| Er | 0·170 ± 0·04 | $Er_2O_3$ | 0·122 9 ± 0·028 9 |
| Tm | 0·009 ± 0·002 | $Tm_2O_3$ | 0·006 4 ± 0·001 4 |
| Yb | 0·04 ± 0·004 | $Yb_2O_3$ | 0·028 0 ± 0·002 8 |
| Lu | 0·004 ± 0·000 4 | $Lu_2O_3$ | 0·002 8 ± 0·000 3 |

The dried powders were deagglomerated by a method described elsewhere[19] and uniaxially compacted under 196 MPa into discs 12 mm diameter and ≃3 mm thickness. Sintering was performed in air at 1250, 1300 and 1350°C for 2 h. The rate of temperature increase was 4°C/min.

The monoclinic phase content in the powders was determined by X-ray diffraction using the method outlined by Porter & Heuer.[20] The phase relations within the sintered samples were assessed by the relative intensities of the particular reflections according to the formulae

$$T = I(111)_T/\Sigma I \quad (1)$$

$$M = I(11\bar{1})_M/\Sigma I \quad (2)$$

$$\Phi_1 + \Phi_2 = [I(222)_{\Phi_1} + I(002)_{\Phi_2} + I(111)_{\Phi_2}]/\Sigma I \quad (3)$$

where

$$\Sigma I = I(111)_T + I(11\bar{1})_M + I(222)_{\Phi_1} + I(002)_{\Phi_2} + I(111)_{\Phi_2}$$

and T, M and $\Phi_1 + \Phi_2$ stand for the relative intensities of indicated reflections of the tetragonal, monoclinic and ordered ($\Phi_1$ and $\Phi_2$) phases, respectively. The method was applied to show the trends of the phase composition changes (including ordered phases) versus stabilizing oxides content at different sintering temperatures.

The (111) line broadening was used to determine the tetragonal and cubic crystallite sizes.[21]

Replica transmission electron micrographs allowed observations of the microstructure and determination of the 'true' grain size distribution by the Saltykov method[22] in the sintered bodies. This information was useful for assessing the critical grain sizes of the tetragonal phase in the sintered body by the procedure shown in Ref. 8. In this case the monoclinic phase content determined by the Porter & Heuer method was used.

Vickers indentations under a load of 196 N applied for 10 s and the Palmqvist crack model[23] were used to determine the fracture toughness ($K_{Ic}$) of the sintered samples. The apparent densities of the sintered ceramic were found by hydrostatic weighing.

## 3 Results and Discussion

### 3.1 Powder characteristics

Data given in Table 2 and Fig. 1 indicate that the powders are composed of isometric ~10 nm crystallites. Monoclinic phase content decreases with the increased stabilizer concentration. Compositions above 4 mol% content of the stabilizing oxide

**Table 2.** Characteristics of powders

| *Stabilizing mixture content (mol%)* | *Monoclinic phase content (vol.%)* | *Crystallite size $D_{111}$ (tetragonal and/or cubic) (nm)* |
|---|---|---|
| 2 | 19·8 ± 0·2[a] | 13·2 |
| 3 | 9·5 ± 0·4 | 12·6 |
| 4 | 2·5 ± 0·2 | 11·8 |
| 5 | 0 | 12·0 |
| 6 | 0 | 10·6 |
| 7 | 0 | 9·8 |
| 8 | 0 | 9·8 |
| 9 | 0 | 10·0 |

[a] ± denotes a confidence interval at a confidence level of 0·95.

mixture show no monoclinic phase content and the tetragonal to cubic phase ratio decreases with the increased stabilizer concentration (see Fig. 2).

### 3.2 Sintered samples characteristics

Phase composition changes of the sintered samples with the stabilizing oxide mixture concentration are shown in Fig. 3. The tetragonal $ZrO_2$ solid solution is the prevailing phase within the samples of the stabilizer contents above 4–5 mol% depending on the sintering temperature. Compositions having the stabilizer concentration within the range of 2–6 mol% reveal some monoclinic phase. In contrast to the results on powders, no cubic phase could be detected within this composition range. However, the diffraction patterns of the compositions of the stabilizing mixture concentration above 3 mol% show some new reflections (see Fig. 4). These reflections were attributed to the ordered phases of the type $Ln_2^{3+}Zr_2O_7$ ($\Phi_1$) and $Ce_2Zr_3O_{10}$ ($\Phi_2$).

The $\Phi_1$ phase, having cubic symmetry and pyrochlore-type structure, has been found in the following systems: $La_2O_3$–$ZrO_2$,[24–28] $Pr_2O_3$–$ZrO_2$,[29] $Nd_2O_3$–$ZrO_2$,[24] $Sm_2O_3$–$ZrO_2$,[30] $Eu_2O_3$–

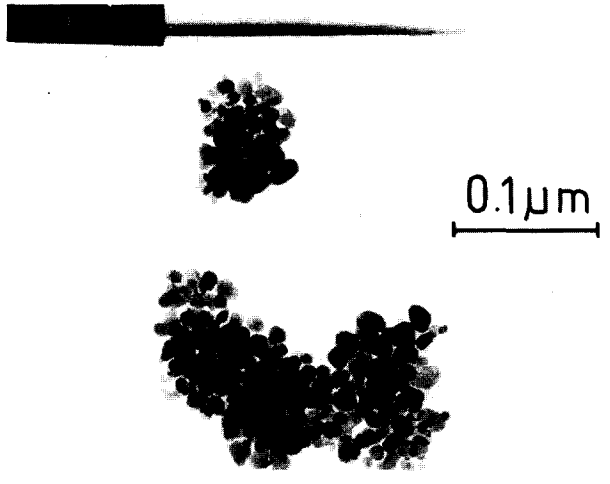


**Fig. 1.** Transmission electron micrograph of the powder with 5 mol% stabilizing oxide mixture additive.

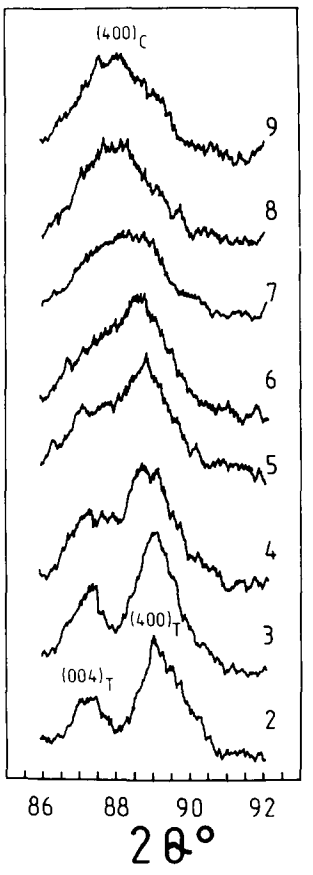


**Fig. 2.** X-Ray diffraction patterns of the powders. Content of the stabilizing oxide mixture indicated. Co$K_\alpha$ radiation.

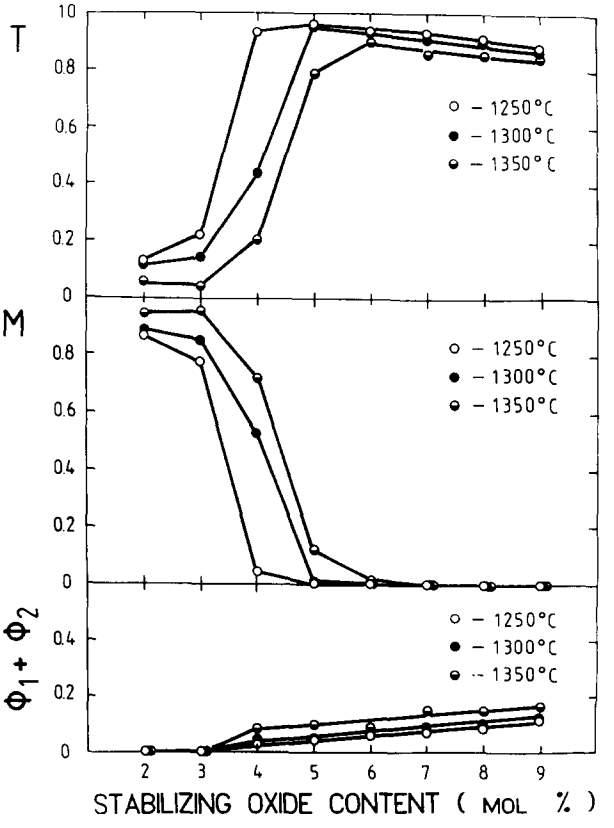


**Fig. 3.** Tetragonal (T), monoclinic (M) and ordered ($\Phi_1 + \Phi_2$) phases content assessed on the basis of eqns (1)–(3). Sintering temperatures indicated.

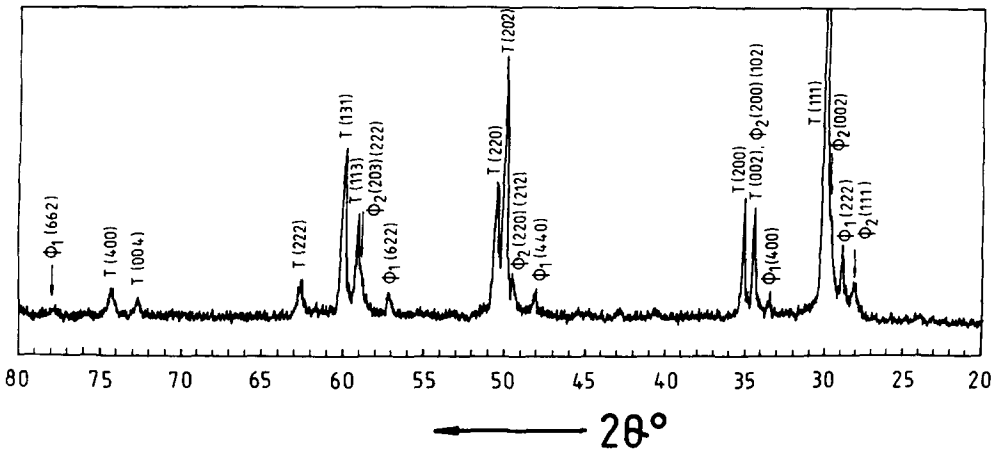


**Fig. 4.** X-Ray diffraction pattern of the sample with 9 mol% stabilizing oxide mixture concentration sintered at 1350°C for 2 h. Cu$K_\alpha$ radiation.

$ZrO_2$[30] and $Gd_2O_3$–$ZrO_2$.[31] $La_2Zr_2O_7$ appears in the system of $La_2O_3$ concentration surpassing ~0·5 mol%,[28] and $Nd_2Zr_2O_7$ appears when the $Nd_2O_3$ content is greater than 4 mol% in the solid solution.[24] These phases are mutually soluble in the solid state. Pyrochlore structures having the formula $Ln_2Zr_2O_7$ are formed when the ionic radii ratio $r_{Ln^{3+}}/r_{Zr^{4+}} \geq 1{\cdot}2$. Hence, Tb, Dy, Ho, Er, Tm, Yb and Lu oxides, present in the mixture studied, should not form this compound as a separate phase. They probably dissolve in $Ln_2Zr_2O_7$ as it occurs in the cases of $Nd_2Zr_2O_7$ and $Gd_2Zr_2O_7$, in which small fractions of Dy can be substituted for Nd or Gd.[25,26] These oxides also dissolve in tetragonal and monoclinic zirconia.

In the system $Y_2O_3$–$ZrO_2$ no ordered phases have been observed in the low yttria concentration region.[32,33]

The $\Phi_2$ phase exists in the $CeO_2$–$ZrO_2$ system.[34–36] A compound of the formula $Ce_2Zr_3O_{10}$ has tetragonal symmetry ($P42_12$) and is stable below 870°C.

The presented data as well as the chemical composition of the stabilizing oxide mixture (see Table 1) indicate that the basic role in the formation of the $\Phi_1$ phase is played by $La_2O_3$, $Nd_2O_3$, $Pr_2O_3$, $Sm_2O_3$, $Gd_2O_3$ and $Eu_2O_3$, and in the case of the $\Phi_2$ phase by $CeO_2$. The remaining oxides probably dissolve in the zirconia and in the $\Phi_1$ and $\Phi_2$ phases. As would be expected, the amount of the $\Phi_1 + \Phi_2$ phases increases with the stabilizing oxides concentration (see Fig. 3).

The monoclinic phase content increases with sintering temperature. This is the behaviour usually encountered in the tetragonal zirconia polycrystals; higher sintering temperatures promote grain growth (see Table 3), causing larger volume fractions of the grains to surpass the critical size. Such grains transform to monoclinic symmetry on cooling. The critical grain sizes depend on the chemical composition of the system. This is also the case for the system studied. Relevant data are presented in Table 3. As is usually observed with the other zirconia systems, the critical grain size increases with the stabilizing oxides concentration. Within the studied composition range it changes from 0·09 to ≥0·31 μm and is considerably smaller than those found in the ceria–zirconia system (1·1–1·9 μm; the critical grain sizes were assessed for the composition of 12% $CeO_2$–$ZrO_2$ by the method described in Ref. 8 using micrographs presented in Ref. 37), although ceria is the major component of the studied stabilizing mixture. The observed critical grain sizes correspond to those in the $Y_2O_3$–$ZrO_2$ system for yttria concentration less than 2 mol% and is comparable with the values found in the Ca–TZP. The data of Table 3 show that the median grain size decreases with the stabilizing mixture concentration, contrary

**Table 3.** Critical grain size ($d_{crit}$) of the tetragonal phase and median grain size ($d_{med}$) of the sintered samples

| *Stabilizing mixture content (mol%)* | *Sintering temperature* | | | |
|---|---|---|---|---|
| | *1300°C* | | *1350°C* | |
| | $d_{crit}$ (μm) | $d_{med}$ (μm) | $d_{crit}$ (μm) | $d_{med}$ (μm) |
| 2 | — | — | 0·09 | 0·25 |
| 3 | — | — | 0·11 | 0·21 |
| 4 | — | — | 0·12 | 0·18 |
| 5 | 0·24 | 0·15 | 0·24 | 0·20 |
| 6 | ≥0·22 | 0·13 | 0·31 | 0·18 |
| 7 | ≥0·23 | 0·13 | ≥0·31 | 0·19 |
| 8 | — | — | ≥0·30 | 0·18 |
| 9 | — | — | ≥0·34 | 0·17 |

Within stabilizer concentrations of 4–6 mol% assessment of $d_{crit}$ is slightly overestimated. This is due to the rough approximation of the $\Phi_1 + \Phi_2$ content.

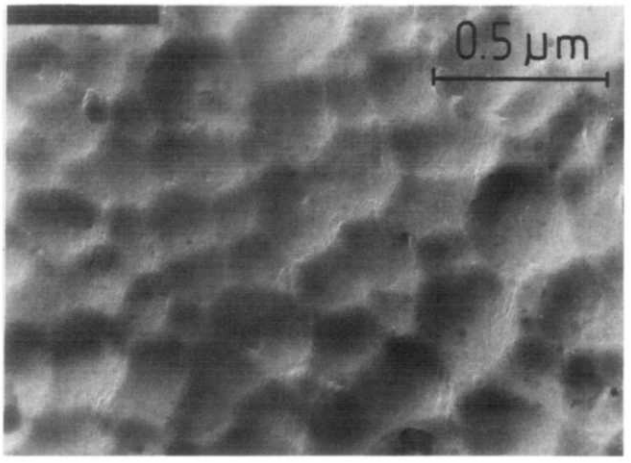


**Fig. 5.** Microstructure of the sample with 5 mol% stabilizing oxide mixture content sintered at 1350°C for 2 h.

to the critical grain sizes. The data has been taken from the electron micrographs similar to that shown in Fig. 5, which is a typical microstructure of the sintered body.

Density measurements (Fig. 6) and water absorption tests (Fig. 7) generally indicate the high densification of the sintered samples. Lower densities and higher water absorptions shown by the samples with low stabilizing oxides concentrations can be attributed to the microcracks related to the tetragonal to monoclinic transformation, which is substantiated by the high monoclinic phase fraction within the low stabilizers concentration range (see Fig. 3). At lower sintering temperatures the samples

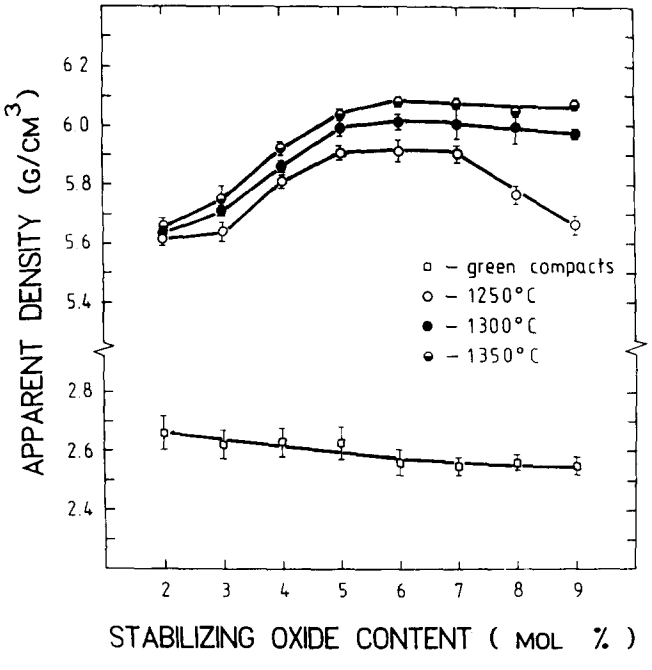


**Fig. 6.** Apparent density of the green compacts and sintered samples versus stabilizing oxide mixture concentration. Sintering temperatures indicated.

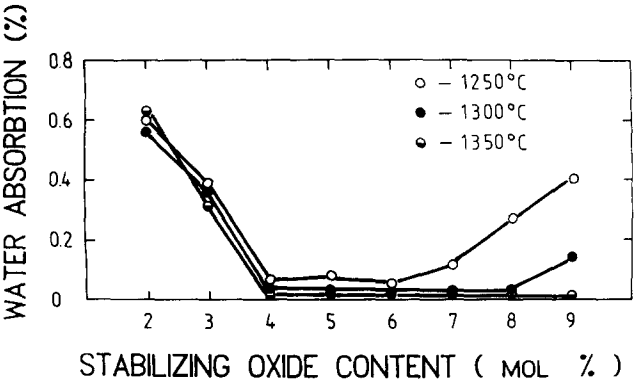


**Fig. 7.** Water absorption of the sintered samples versus stabilizing oxide mixture concentration. Sintering temperatures indicated.

with the highest stabilizing oxides concentration have relatively low densities (Fig. 6) and open porosity, indicated by the marked water absorption (Fig. 7). It is worth noting that a similar phenomenon was also observed in the $CaO–ZrO_2$ system;[38] in this case densification of the samples has been lower with the higher concentration of the stabilizing oxide.

Figures 8 and 9 demonstrate the effect of sintering temperature and chemical composition on fracture toughness ($K_{Ic}$) and hardness ($H_V$) of the studied materials. Materials having the best fracture toughness can be prepared within the stabilizing oxide mixture concentration in the range 5–7 mol%. Further increase of the stabilizer concentration decreases the $K_{Ic}$ value. This effect can be attributed to the decreasing transformability of the tetragonal

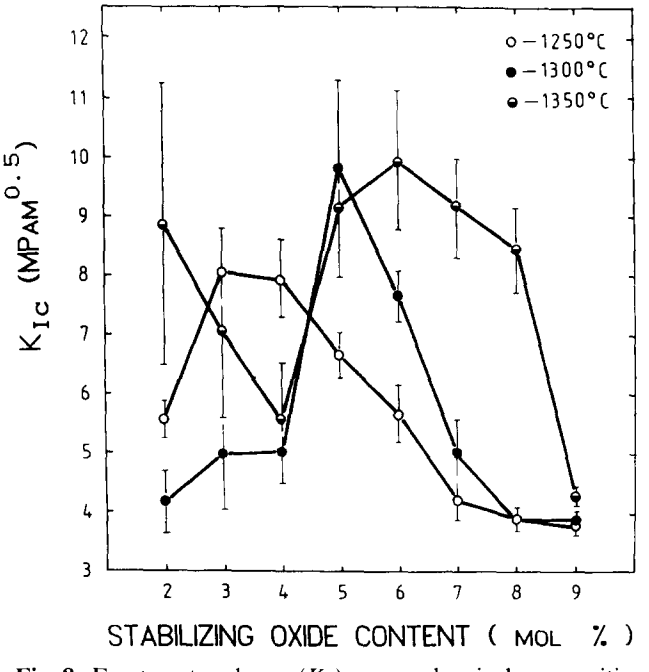


**Fig. 8.** Fracture toughness ($K_{Ic}$) versus chemical composition. Sintering conditions indicated.

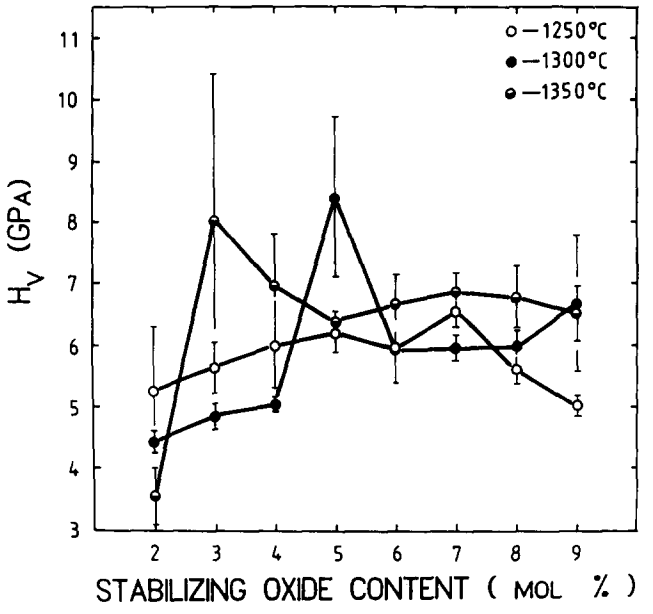


**Fig. 9.** Vickers hardness ($H_V$) versus chemical composition. Sintering conditions indicated.

phase, the effect shown in the $Y_2O_3$–$ZrO_2$ system.[3] It cannot be excluded that the increasing 'dilution' of the system with the stabilizing mixture concentration as well as the presence of the untransformable $\Phi_1$ and $\Phi_2$ phases (see Fig. 3) is another factor which contributes to the material, showing a decrease in toughness.

Low hardness of the samples with the lowest stabilizers concentration can be explained by the microcrack porosity (*c.* Fig. 7), and the authors found that the samples of the highest stabilizers concentration sintered at 1250°C do not achieve full densification, so they show low hardness.

## 4 Conclusions

It has been shown that using the phosphogypsum as a source for the mixture of the rare earth oxides and yttria additives it is possible to obtain tetragonal zirconia polycrystals with good mechanical properties. The best results have been obtained within the range of 5–7 mol% stabilizer concentration.

The small critical grain sizes of the tetragonal phase (0·09 to $\geq$0·31 $\mu$m) allow powders of good sintering ability to be utilized. Hydrothermal crystallization was a suitable method for the preparation of such powders.

Chemical segregation occurs with compositions of stabilizing mixture content $\geq$3 mol%. $Ln_2Zr_2O_7$ and $Ce_2Zr_3O_{10}$ ordered phases coexisting with the tetragonal zirconia solid solution were identified. The relative content of these phases increases with the stabilizing mixture concentration.

## References


1. Gupta, T. K., Sintering of tetragonal zirconia and its characteristics. *Sci. Sintering*, **10** (1978) 205.
2. Gupta, T. K., Bechtold, J. H., Kuznicki, R. C., Cadoff, R. H. & Rossing, B. R., Stabilization of tetragonal phase in polycrystalline zirconia. *J. Mat. Sci.*, **12** (1977) 2421.
3. Haberko, K. & Pampuch, R., Influence of yttria content on phase composition and mechanical properties of Y-TZP. *Ceram. Int.*, **9** (1983) 8.
4. Tsukuma, K. & Shimada, M., Strength, fracture toughness and Vickers hardness of Ce-stabilized tetragonal zirconia polycrystals (Ce-TZP). *J. Mat. Sci.*, **20** (1985) 1178.
5. Tsukuma, K., Mechanical properties and thermal stability of $CeO_2$ containing tetragonal zirconia polycrystals. *Am. Ceram. Soc. Bull.*, **65** (1986) 1386.
6. Meriani, S., Zirconia–ceria ceramics research and development. In *Proc. 12th Int. Technical Colloquium on Ceramics Processing*, Rimini, September 1987; for abstract see *Ceramurgia*, **16** (1987) 206.
7. Coyle, T. W., Coblenz, W. S. & Bender, B. A., Transformation toughening in large-grain-size $CeO_2$-doped $ZrO_2$. *J. Am. Ceram. Soc.*, **71** (1988) C-88.
8. Pyda, W. & Haberko, K., CaO-containing tetragonal $ZrO_2$ polycrystals (CaO–TZP). *Ceram. Int.*, **13** (1987) 113.
9. Haberko, K., Pyda, W., Kuraś, M. & Bućko, M., Tetragonal zirconia polycrystals in the MgO–$Y_2O_3$–$ZrO_2$ system (MgY–TZP). In *Advances in Zirconia Science and Technology—Zirconia '88*, ed. S. Meriani & C. Palmonari. Elsevier Applied Science, London, 1989, pp. 107–18.
10. Haberko, K. & Pyda, W., Tetragonal zirconia polycrystals in the MgO–$Y_2O_3$–$ZrO_2$ system—their preparation and properties. In *UNITECR '89 Proceedings*, Vol. 2, ed. L. J. Trostel Jr. American Ceramic Society, Columbus, OH, 1989, pp. 1679–93.
11. Lee, R. R. & Heuer, A. H., Morphology of tetragonal $ZrO_2$ in a ternary (Mg,Y)-PSZ. *J. Am. Ceram. Soc.*, **70** (1987) 208.
12. Biswas, N. C. & Chakravorty, D., Mechanical properties of multi-phase ceramics in the CaO–$TiO_2$–$ZrO_2$ system. *J. Mat. Sci. Lett.*, **1** (1982) 119–20.
13. Hofmann, H., Michel, B. & Gauckler, L. J., Zirconia powder for TZP-ceramics, Ti–Y-TZP. In *Advances in Zirconia Science and Technology—Zirconia '88*, ed. S. Meriani & C. Palmonari. Elsevier Applied Science, London, 1989, pp. 119–29.
14. Haberko, K., Pyda, W. & Bućko, M. M., Zirconia polycrystals in the system $TiO_2$–$Y_2O_3$–$ZrO_2$. In *Materials Science Monographs, Series 66C, Proc. 7th International Meeting on Modern Ceramics Technologies, 7th CIMTEC—World Ceramic Congress*, Montecatini Terme, Italy, 24–26 June 1990, ed. P. Vincenzini. Elsevier, Amsterdam–Oxford–New York–Tokyo, 1991, pp. 1563–72.
15. Haberko, K., Pyda, W. & Bućko, M. M., Polikryształy dwutlenku cyrkonu domieszkowane $TiO_2$ i $Y_2O_3$ (Zirconia polycrystals doped with $TiO_2$ and $Y_2O_3$). *Inż. Mater.*, **11** (1990) 120–4.
16. Haberko, K., Pyda, W., Bućko, M. M. & Faryna, M., Tough materials in the system $TiO_2$–$Y_2O_3$–$ZrO_2$. In *Proc. European Ceramic Society Second Conference*, Augsburg, Germany, September 1991, in print.
17. Kijkowska, R., Recovering rare earth elements from Kola apatite and Moroccan phosphate rock. *Phosphorus & Potassium*, No. 127 (1983) 24–6.
18. Haberko, K. & Pyda, W., Preparation of Ca-stabilized $ZrO_2$ micropowders by a hydrothermal method. In *Advances in Ceramics*, Vol. 12, ed. N. Claussen, M. Rühle & A. H. Heuer. American Ceramic Society, Columbus, OH, 1984, pp. 774–83.
19. Pyda, W. & Haberko, K., Behaviour of ceramic micropowders during dry compaction and sintering. In *Materials*

*Science Monographs, Series 66B, Proc. 7th International Meeting on Modern Ceramics Technologies, 7th CIMTEC—World Ceramic Congress*, Montecatini Terme, Italy, 24–26 June 1990, ed. P. Vincenzini. Elsevier, Amsterdam–Oxford–New York–Tokyo, 1991, pp. 1023–32.
20. Porter, D. L. & Heuer, A. H., Microstructural development in MgO-partially stabilized zirconia (Mg-PSZ). *J. Am. Ceram. Soc.*, **62** (1979) 298.
21. Klug, H. P. & Alexander, L. E., In *X-Ray Diffraction Procedures for Polycrystalline and Amorphous Materials*, 2nd edn. J. Wiley & Sons, New York, 1974, Chapter 9.
22. Saltykov, S. A., *Stereometric Metallography*, 3rd edn. Metallurgija, Moskwa, 1970 (in Russian).
23. Niihara, K. A., A fracture mechanics analysis of indentation-induced Palmqvist crack in ceramics. *J. Mat. Sci. Lett.*, **2** (1983) 221.
24. Roth, R. S., *J. Res. Natl Bur. Standards*, **56** (1956) 17–25.
25. Collongues, R., Les phénomènes d'ordre–désordre en chimie minérale. *Ann. Chim.*, **8** (1963) 395–408.
26. Collongues, R., Phénomènes d'ordre–désordre en métallurgie et en chimie minérale. *Silicates Industriels*, **31** (1966) 399–410.
27. Rouanet, A., Zirconia–lanthanide oxide systems. *Rev. Int. Hautes Temp. Refract.*, **2** (1971) 161–80.
28. Bastide, B., Odier, P. & Coutures, J. P., Phase equilibrium and martensitic transformation in lanthana-doped zirconia. *J. Am. Ceram. Soc.*, **71** (1988) 449–53.
29. Pâris, G., Szabo, G. & Pâris, R. A., Sur l'obtention des zirconates de métaux bivalents et trivalents. *C.R. Acad. Sci. Paris*, **266C** (1968) 554–6.
30. Berry, L. G. (ed.), In *Joint Committee on Powder Diffraction Standards*, Swarthmore, Pennsylvania, USA, 1976, Tables 24-1012, 24-418.
31. Duran, P., The system erbia–zirconia. *J. Am. Ceram. Soc.*, **60** (1977) 510–13.
32. Scott, H. G., Phase relationships in the zirconia–yttria system. *J. Mat. Sci.*, **10** (1975) 1527–35.
33. Pascual, C. & Duran, P., Subsolidus phase equilibria and ordering in the system $Zr_2O$–$Y_2O_3$. *J. Am. Ceram. Soc.*, **66** (1983) 23–7.
34. Roitti, S. & Longo, V., Investigation of phase equilibrium diagrams among oxides by means of electrical conductivity measurements. Application of the method to the system $CeO_2$–$ZrO_2$. *Ceramurgia*, **2** (1972) 97–102.
35. Longo, V. & Minichelli, D., X-Ray characterization of $Ce_2Zr_3O_{10}$. *J. Am. Ceram. Soc.—Discussions and Notes*, **56** (1973) 600.
36. Duran, P., Gonzalez, M., Moure, C., Jurado, J. R. & Pascual, C., A new tentative phase equilibrium diagram for the $ZrO_2$–$CeO_2$ system in air. *J. Mat. Sci.*, **25** (1990) 5001–6.
37. Duh, J. G., Dai, H. T. & Chiou, B. S., Sintering, microstructure, hardness and fracture toughness behaviour of $Y_2O_3$–$CeO_2$–$ZrO_2$. *J. Am. Ceram. Soc.*, **71** (1988) 813–19.
38. Garvie, R. C., Zirconium dioxide and some of its binary systems. In *High Temperature Oxides, Part II*, ed. A. M. Alper, Academic Press, New York–London, 1970, pp. 117.